



## Is there a correlation between the glass forming ability of a drug and its supersaturation propensity?



Lasse Ingerslev Blaabjerg<sup>a</sup>, Eleanor Lindenberg<sup>b</sup>, Korbinian Löbmann<sup>a,\*</sup>, Holger Grohgan<sup>a</sup>, Thomas Rades<sup>a</sup>

<sup>a</sup> Department of Pharmacy, University of Copenhagen, Universitetsparken 2, 2100 Copenhagen, Denmark

<sup>b</sup> Idorsia Pharmaceuticals Ltd, Heggenheimermattweg 91, CH-4123 Allschwil, Switzerland

### ARTICLE INFO

#### Keywords:

Amorphous  
Supersaturation  
Precipitation  
Glass forming ability

### ABSTRACT

The use of an enabling formulation technique, such as amorphization of a poorly water-soluble crystalline drug, can result in supersaturation with respect to the crystalline form of the drug and thus potentially in a higher degree of absorption after oral administration. The ease with which such drugs can be amorphized is known as their glass forming ability (GFA). In this study, a potential correlation between GFA and supersaturation propensity is investigated. The GFA of 23 different drugs was determined by melt quenching or milling the crystalline drugs to obtain their respective amorphous forms. The inherent propensity of the drug to supersaturate, i.e. the maximal apparent degree of supersaturation (aDS), and the time until precipitation at a given aDS were determined. Supersaturation was induced via a solvent shift method where the drug was initially dissolved in dimethyl sulfoxide and then added to a biorelevant medium (fasted state simulated intestinal fluid). The study showed that drugs which are good glass formers also have the potential to supersaturate to a high degree (high maximal aDS) whereas drugs that are modest glass formers supersaturate only to a low degree. This correlation was confirmed by principal component analysis, which also indicated that melt enthalpy inversely correlated with both GFA and maximal aDS. However, no correlation between GFA of a drug and the time until precipitation at a given aDS was found.

### 1. Introduction

The growing number of drug candidates in the pipelines of the pharmaceutical industry that show poor aqueous solubility is a major drug development challenge (Di et al., 2009). Poor aqueous solubility may result in low bioavailability and otherwise promising drug candidates may suffer from long development times or may even be discarded (Kalepu and Nekkanti, 2015). One way to improve aqueous solubility is the transformation of a crystalline drug candidate into an amorphous form, thereby increasing its apparent solubility (Hancock and Parks, 2000). The ease of amorphization, or glass forming ability (GFA), of a drug is usually characterized by the critical cooling rate (Baird et al., 2010; Blaabjerg et al., 2016). The Taylor group proposed a classification system to assess and categorize the GFA of drugs based on their recrystallization tendency during cooling and heating cycles. It was proposed that drugs, which recrystallized during cooling of the melt at 20 K/min belonged to class 1T, whereas class 2T drugs did not recrystallize during cooling of the melt at 20 K/min, but recrystallized in the following heat cycle at 10 K/min. Finally, class 3T drugs neither

recrystallized during cooling of the melt at 20 K/min nor during the following heat cycle at 10 K/min (Baird et al., 2010). Classes 1T, 2T and 3T represent poor, modest and good glass formers, respectively. A later study from our group revealed that drugs could be classified according to their inherent crystallization tendency during melt quenching and a new classification system was proposed (Blaabjerg et al., 2016). Here, drugs belonging to class 1R could not be made fully amorphous by melt quenching even when using a cooling rate of 750 K/min from the melt. Class 2R drugs could be made amorphous at a critical cooling rate of about 10–20 K/min. Finally, class 3R drugs turned amorphous even when cooling the melt at a cooling rate of only about 0.5–2 K/min during melt quenching (Blaabjerg et al., 2016). This classification system using melt quenching was later correlated with the amorphization behavior of the drugs during milling, using a vibrational ball mill (Blaabjerg et al., 2017). It was found that drugs belonging to class 1R could not turn amorphous even when milled for 360 min at temperatures below the glass transition temperature ( $T_g$ ) of the drug. Class 2R drugs turned amorphous when milled between 180 and 270 min and class 3R drugs turned amorphous when milled for less than 90 min.

\* Corresponding author.

E-mail address: [korbinian.loebmann@sund.ku.dk](mailto:korbinian.loebmann@sund.ku.dk) (K. Löbmann).

The dissolution of an amorphous form of a drug may give rise to a “spring effect” as the drug quickly generates a supersaturated state, with respect to the equilibrium solubility of the most stable crystalline form of the drug (Guzman et al., 2007). However, this may be followed by rapid precipitation, which limits potential absorption benefits of the initially generated supersaturation. Precipitation is essentially a result of nucleation and crystal growth as the drug is in a thermodynamically unfavorable state when supersaturated. This means that for a given drug, a higher degree of supersaturation (DS) increases the risk of precipitation (Palmelund et al., 2016). During precipitation, the drug may crystallize to a metastable form (Sudha and Srinivasan, 2013), which still possesses a higher apparent solubility than the equilibrium solubility of the stable crystalline form or to a hydrate form that possesses a lower equilibrium solubility than the stable crystalline form (Tian et al., 2006).

Several studies on supersaturation and precipitation of drugs can be found in the literature (Gao and Shi, 2012; Li et al., 1998; Palmelund et al., 2016; Wu and Khan, 2011). The studies differ in the way supersaturation is induced and the way precipitation is detected. Supersaturation of a drug has for example been studied by powder dissolution of amorphous solids (Hancock and Parks, 2000). The maximal DS however, may depend on the way the amorphous form is generated, as the preparation method can influence physical stability and dissolution rate of the drug (Karmwar et al., 2011, 2012). Supersaturation can also be induced by a pH shift or solvent shift method, i.e. by using the drug in a dissolved form. The pH shift method induces supersaturation via dissolving the ionized form of a drug which is then titrated to obtain the neutral form; thus, this method is only suitable for ionizable compounds. In the solvent shift method, the drug is dissolved in a solvent in which it is highly soluble and then transferred into an acceptor medium where the drug has a low solubility to acquire supersaturation. In contrast to the powder dissolution of an amorphous solid and the pH shift method, the solvent shift method is easy to use and requires only that the compound is much more soluble in the organic phase compared to the (aqueous) acceptor medium and that the organic solvent is miscible with the acceptor medium. Commonly, an arbitrary potential DS (i.e. an arbitrary starting concentration of the drug in the organic phase) is chosen when investigating the supersaturation propensity of a drug by solvent shift (Ozaki et al., 2012; Van Eerdenbrugh et al., 2014).

Palmelund et al. (2016) recently proposed a generally applicable approach to investigate the inherent supersaturation propensity of a drug, i.e. the maximal DS and the relationship between various DS and the time until precipitation at these DS. Here, the drug is dissolved in an organic medium, in which it is highly soluble, and titrated into an acceptor medium in which the drug is much less soluble. As titration of the drug into the acceptor medium will eventually result in precipitation of the drug, the maximal DS, i.e. the potential of the drug to supersaturate, is determined as the concentration at which precipitation occurs during titration. Three lower concentrations are additionally tested relative to the maximal DS, and the times to precipitation are determined (Palmelund et al., 2016). This method uses only a small amount of organic solvent (2.0% dimethyl sulfoxide concentration in the resulting aqueous medium), which is beneficial, as increasing dimethyl sulfoxide concentrations often increase solubility of the drug in the acceptor media (Van Speybroeck et al., 2010). Furthermore, biorelevant media, e.g. in form of fasted state simulated intestinal fluid (FaSSIF), can also be used instead of a buffered solution in the solvent shift method (Palmelund et al., 2016). This method, which allows the determination of a drug’s inherent supersaturation propensity, is used in the current study.

The DS is defined as the ratio between the activity of the dissolved species in the supersaturated solution and the activity of the species in a saturated solution (Mullin and Söhnel, 1977). However, the thermodynamic activity of a drug in a supersaturated FaSSIF solution is difficult to determine since the drug may become molecularly dispersed or incorporated into micelles or other colloidal species present in FaSSIF.

Therefore, the concentration of the (solubilized and molecularly dispersed) drug is used instead of the activity to calculate an apparent degree of supersaturation (aDS):

$$aDS = C_{\text{supersaturation}}/C_{\text{equilibrium}} \quad (1)$$

where  $C_{\text{supersaturation}}$  is the concentration of the drug in a supersaturated solution and  $C_{\text{equilibrium}}$  is the concentration of the drug in a saturated solution.

Several studies have attempted to predict the solubility and dissolution rate advantages of amorphous compounds (Hancock and Parks, 2000; Murdande et al., 2010, 2011; Almeida e Sousa et al., 2015). Hancock and Parks (2000) found that it is rather difficult to predict the solubility advantage, as the underlying mechanisms of crystallization of amorphous compounds are still not fully understood. This was also experienced by Murdande et al. (2010, 2011), who found that the properties of the amorphous drug change significantly in the presence of water and that thermal history may play a role in the onset of recrystallization. Finally, Almeida e Sousa et al. (2015) had limited success with predicting the solubility increase of the amorphous form compared to the crystalline form via the difference in Gibbs free energy between the two forms using the Hoffman equation (Hoffman, 1958):

$$\Delta G = (\Delta H_{\text{fus}} \cdot (T_m - T) \cdot T) / T_m^2 \quad (2)$$

where  $\Delta G$  is the change in Gibbs free energy upon recrystallization,  $\Delta H_{\text{fus}}$  is the enthalpy of fusion,  $T_m$  is the melting point of the crystalline compound and  $T$  is temperature.

Other studies have attempted to correlate the GFA of a drug with its propensity to supersaturate. Van Eerdenbrugh et al. (2014) proposed a classification system based on the time required until crystallization of the drug in a supersaturated solution occurred. Supersaturation was induced using a solvent shift method by adding a fixed concentration (100 mg/ml) of the drug dissolved in dimethyl sulfoxide to an aqueous buffer. Synchrotron radiation was used to monitor the crystallization of the drug. The study categorized 50 different drugs into three classes: class 1 drugs crystallized within 150 s, class 2 drugs within 1 h and class 3 drugs did not crystallize within 1 h. The study correlated these classes with the above mentioned classification system of GFA by Baird et al. and found that approximately 60% of the investigated drugs fell into the same class in the two proposed classification systems (Baird et al., 2010; Van Eerdenbrugh et al., 2014). Raina et al. (2015) also applied the solvent shift method to induce supersaturation of six different drugs at a fixed concentration (100 mg/ml) in phosphate buffer and proposed another classification system using four categories: *Fast drugs* crystallized within 15 min, *moderate-fast* drugs within 3 h, *moderate-slow* drugs within 6 h and *slow* drugs between 6 and 12 h (Raina et al., 2015), which did not directly correlate with the classification system of GFA proposed by Baird et al. (2010).

In this study, the inherent GFA of a range of drugs was determined by melt quenching or milling using the methods described by Blaabjerg et al. (2016, 2017). The inherent supersaturation propensity was determined by the use of the above described solvent shift method by Palmelund et al. (2016). The study on the one hand investigated the correlation between GFA of the drugs and their potential to supersaturate, i.e. the maximal aDS of the drugs, and on the other hand the correlation between GFA and the time until precipitation at various aDS.

## 2. Materials and methods

### 2.1. Materials

Carbamazepine, flurbiprofen, furosemide, ibuprofen, itraconazole, naproxen, phenytoin and tolbutamide were obtained from Chemie Brunschwig (Basel, Switzerland). Celecoxib was obtained from Dr. Reddy’s (Hyderabad, India). Tolfenamic acid was obtained from Combi-Blocks Inc. (San Diego, USA). Mefenamic acid was obtained from

Bepharm Ltd. (Shanghai, China). Clotrimazole was obtained from Fagron A/S (Copenhagen, Denmark). Albendazole, cinnarizine, flufenamic acid, griseofulvin, ketoconazole and probenecid, sodium chloride, sodium hydroxide and sodium phosphate dihydrate were obtained from Sigma-Aldrich (Steinheim, Germany). Aprepitant (Merck, Kenilworth, USA), danazol (Sanofi Aventis, Paris, France), felodipine (AstraZeneca, London, United Kingdom), fenofibrate (Veloxis, Hørsholm, Denmark), and tadalafil (Eli Lilly, Indianapolis, USA) were gifted from the respective companies. All drugs were used as received. Dimethyl sulfoxide was obtained from VWR Chemicals (Søborg, Denmark). SIF powder was obtained from Biorelevant (South Croydon, United Kingdom).

## 2.2. Determination of thermal stability

Thermogravimetric analysis was used to study the thermal stability of the drugs upon melting. Approximately 10 mg of the raw material was placed into a platinum pan and heated from 298 K to 573 K at a rate of 10 K/min using a TGA Discovery (TA Instrument, New Castle, USA). The resulting thermograms were analyzed by the use of the Trios software (TA-instruments-waters LLC, New Castle, USA) to calculate the weight loss between 298 K and  $T_m + 20$  K.

## 2.3. Determination of glass transition temperature, melting point and melt enthalpy

Differential scanning calorimetry (DSC) was performed using a DSC 8500 (PerkinElmer, Zürich, Switzerland). The sample was weighed into an aluminium pan and sealed with an aluminium lid. The furnace was flushed with dry nitrogen at a flow rate of 20 mL/min. The melting point onset ( $T_m$ ) and melt enthalpy were determined by heating the sample at a rate of 2 K/min in the range of  $\pm 25$  K of the peak melting temperature. To determine the glass transition temperature ( $T_g$ ), the sample was held 10 K above its melting point for 3 min, then cooled at a ballistic rate ( $> 750$  K/min) to 213 K before being heated at 10 K/min from 213 to 20 K above the melting point. The  $T_g$  was calculated as the midpoint between the onset and endset temperature of the step change in the thermogram. Melt enthalpy,  $T_g$  and  $T_m$  were determined from three independent samples. Data analysis was performed using the Pyris software version 11.0.0.0449 (PerkinElmer, Zürich, Switzerland).

## 2.4. Determination of glass forming ability by melt quenching

Amorphous drugs were prepared by melt quenching as reported earlier (Blaabjerg et al., 2016). Data analysis was performed using the Pyris software version 11.0.0.0449 (PerkinElmer, Zürich, Switzerland). The experiments were conducted in triplicate.

## 2.5. Determination of glass forming ability by vibrational ball milling

Amorphous albendazole was prepared by vibrational ball milling as reported earlier (Blaabjerg et al., 2017). Vibrational ball milling (Mixer Mill 400, Retsch GmbH & Co., Haan, Germany) was used to mill a total mass of 1500 mg of the crystalline compound in 25 mL milling jars with two 12 mm stainless steel balls at a milling frequency of 30 Hz for up to 360 min at ambient conditions. Samples were withdrawn at various time points (90, 180, 270 and 360 min) and analyzed by X-ray powder diffraction (XRPD). XRPD patterns were collected using a previously described method (Blaabjerg et al., 2017). The diffraction patterns were obtained in reflectance mode on a Bruker D8 GADDS-HTS diffractometer (Bruker AXS GmbH, Karlsruhe, Germany) using Cu K $\alpha$  radiation (40 kV, 40 mA), an automated XYZ stage, a laser video microscope for auto-sample positioning and a Vantec-500 detector. X-ray optics consisted of a single Göbel multilayer mirror coupled with a pinhole collimator of 0.5 mm. The samples were gently pressed on a glass slide to obtain a flat surface and analyzed under ambient

conditions. The goniometer positions were Theta1 7° and Theta2 9°, the detector distance 20 cm and the integration frame between 5 and 35° 2 $\theta$  using a step size of 0.020° 2 $\theta$ . Data analysis was performed using DIFFRAC. Suite Eva V4.1 software (Bruker AXS GmbH, Karlsruhe, Germany). All experiments were conducted in duplicate.

## 2.6. Preparation of FaSSiF

FaSSiF was prepared from a commercially available SIF powder as specified by the manufacturer (Biorelevant, South Croydon, United Kingdom). Phosphate buffer was prepared with 3.954 mg/mL of monobasic sodium phosphate, 0.420 mg/mL of NaOH, and 6.186 mg/mL of NaCl dissolved in purified water (SG Ultra Clear UV 2002, Evoqua water Technologies LLC, Barsbüttel, Germany) and adjusted to pH 6.5 using either 1 M NaOH or 1 M HCl. SIF powder was dissolved (2.24 mg/mL) in the phosphate buffer and stirred for 2 h at ambient temperature before use.

## 2.7. Determination of the equilibrium solubility

The equilibrium solubility of the investigated compounds was determined using a  $\mu$ -dissolution set-up ( $\mu$ -DISS Profiler™, Pion, Billerica, MA) at 310 K using the experimental settings shown in Supplementary Table S1. An excess amount of the crystalline drug was added to the vessels containing FaSSiF. The equilibrium solubility was taken as the plateau reached during dissolution, no later than 24 h into the experiment. The drug concentration was additionally confirmed by filtering the sample using a 0.25  $\mu$ m cellulose acetate Q-MAX® RR syringe filter (Frisenette Aps, Knebel, Denmark) to remove all particles in the media, which may interfere with the *in-situ* UV measurements due to light scattering. The experiments were conducted using six replicates for each drug.

## 2.8. Determination of the supersaturation propensity

Supersaturation of the drugs in FaSSiF was induced using a solvent shift method developed previously (Palmelund et al. 2016). The concentration of the drug in the stock solution, named  $C_{ss,100\%}$  was found by determining the maximal concentration in the acceptor media before precipitation. Standard curves for all drugs were prepared by adding aliquots (20–50  $\mu$ L) of the drug dissolved in DMSO (1–50 mg/mL) into FaSSiF until immediate precipitation was observed. Precipitation was detected by a shift in the baseline of the UV spectrum, diversion from linearity between absorbance and concentration of the drug and by visual inspection. Three other stock solutions were made from  $C_{ss,100\%}$  at 87.5, 75 and 50% of the concentration of  $C_{ss,100\%}$ , respectively.

The four stock solutions were used to induce supersaturation in FaSSiF. 200  $\mu$ L of stock solution was spiked into 10 mL FaSSiF (310 K), and stirred with a cross bar magnet at  $100 \pm 3$  rpm. The concentration of the drug in solution was measured *in-situ* using the second derivative of the UV-absorbance in the  $\mu$ -DISS Profiler until precipitation occurred (or for a maximum of 24 h). The second derivative of the UV-absorbance was used to minimize the interference from particle light scattering. The induction time  $t_{ind}$  was taken as the time at which the concentration of the supersaturated solution had decreased by 2.5%. The experiment was conducted for each drug and stock solution concentration using six replicates.

Using this method, the inherent supersaturation propensity of a drug can be evaluated by determination of the maximal aDS and the time until precipitation at various aDS.

## 2.9. Multivariate data analysis

Principal component analysis was performed using Latentix version 2.12 software (LatentiX, Frederiksberg, Denmark). All variables were unit variance-scaled. The variables melting point, melt enthalpy,

**Table 1**M<sub>w</sub>, T<sub>m</sub>, T<sub>g</sub>, H<sub>fus</sub>, GFA class, critical cooling rate and pKa of the investigated drugs.

Drug	Molecular weight (g/mol)	T <sub>m</sub> (K)	T <sub>g</sub> (K)	ΔH <sub>fus</sub> (kJ/mol)	GFA class	Critical cooling rate (K/min)	pKa (acid/basic)
Albendazole	265.34	482.3 (± 1.1)	333	–	3R	– <sup>a</sup>	5.4/10.7
Aprepitant	534.43	526.5 (± 0.0)	368	103.3 (± 1.5)	3R	1	4.4/8.1
Carbamazepine	236.27	464.9 (± 0.1)	306	105.0 (± 1.6)	3R	2	13.9
Celecoxib	381.38	432.5 (± 0.2)	323	97.9 (± 0.2)	2R	20	9.7
Cinnarizine	368.52	388.8 (± 0.4)	288	105.6 (± 2.1)	3R	1	6.1
Clotrimazole	344.84	418.1 (± 0.0)	303	100.5 (± 1.4)	3R	2	13.1
Danazol	337.46	499.9 (± 0.1)	369	96.6 (± 3.0)	3R	1	3.0/9.1
Felodipine	384.26	418.2 (± 1.7)	318	85.5 (± 0.6)	3R	1	2.7
Fenofibrate	360.84	352.7 (± 0.0)	255	97.9 (± 0.7)	3R	1	–
Flufenamic acid	281.23	406.5 (± 0.0)	284	104.2 (± 0.5)	2R	15	3.7
Flurbiprofen	244.26	383.5 (± 0.4)	281	111.1 (± 0.9)	2R	15	4.1
Furosemide	330.75	483.7 (± 1.0)	351	139.5 (± 2.0)	2R	20	3.0/ 9.8
Griseofulvin	352.77	493.2 (± 0.1)	363	113.7 (± 1.2)	3R	1	–
Ibuprofen	206.28	345.2 (± 0.2)	228	124.6 (± 0.2)	3R	2	4.4
Itraconazole	705.65	434.7 (± 0.1)	332	80.8 (± 1.1)	3R	1	2.9/3.6/6.5
Ketoconazole	531.44	422.4 (± 0.8)	319	104.8 (± 1.8)	3R	1	3.6/6.9
Mefenamic acid	241.29	503.3 (± 0.2)	–	141.2 (± 1.6)	1R	> 750	3.7
Naproxen	230.26	430.9 (± 0.2)	278	135.2 (± 0.5)	1R	> 750	4.8
Phenytoin	252.27	570.9 (± 0.4)	–	134.5 (± 3.6)	1R	> 750	8.3
Probenecid	285.36	472.3 (± 0.4)	–	150.8 (± 1.8)	1R	> 750	3.7
Tadalafil	389.41	572.6 (± 0.5)	416	105.17 (± 0.6)	3R	1	–
Tolbutamide	270.35	407.6 (± 0.1)	276	95.9 (± 0.2)	2R	20	5.3
Tolfenamic acid	261.71	480.3 (± 0.4)	–	138.8 (± 0.6)	1R	> 750	3.7

<sup>a</sup> Minimal milling time of 85 min.

critical cooling rate, classification of glass forming ability (class 1R, class 2R and class 3R), equilibrium solubility and maximal aDS were determined as stated above and shown in Table 1. Theoretical pKa values of the drugs were determined by the software pKa dB version 12 (ACD labs, Toronto, Canada) (Table 1).

### 3. Results and discussion

#### 3.1. Determination of glass forming ability

The GFA of a drug can be classified experimentally by melt quenching or milling (Blaabjerg et al., 2016, 2017). For classification using melt quenching, the thermal stability upon melting of 23 selected drugs was initially investigated by thermogravimetric analysis. All drugs, except for albendazole, degraded by less than 5% (w/w) upon melting (data not shown) and were therefore deemed suitable for classification by melt quenching. Albendazole degraded by more than 10% (w/w) upon melting and was therefore classified using the vibrational ball milling approach (Blaabjerg et al., 2017).

In this study GFA classes 1R, 2R and 3R were represented by five, five and thirteen drugs, respectively as shown in Table 1. These findings are in line with previous studies reported by our group (Blaabjerg et al. 2016, 2017). For the study of supersaturation propensity, the drugs belonging to class 1R (mefenamic acid, naproxen, phenytoin, probenecid, tolfenamic acid) were excluded, as formation of their respective amorphous form was not possible. No studies in the literature reporting supersaturation of these drugs without excipients were found.

#### 3.2. Correlation between GFA and apparent degree of supersaturation

The apparent degree of supersaturation (aDS) for six of the selected drugs has earlier been described in the literature (Palmelund et al., 2016). The apparent degree of supersaturation of the remaining twelve drugs was therefore investigated by the use of the same solvent shift method using a μ-dissolution set-up (Palmelund et al., 2016).

The equilibrium solubility of the drugs in FaSSiF was determined in order to calculate the aDS. Table 2 summarizes the solubility data, which is in line with previous findings in the literature (Augustijns et al., 2014; Fagerberg et al., 2015). The inherent potential of the drugs to supersaturate was investigated using four different aDS, including

the maximal aDS. The aDS of the investigated drugs were calculated using Eq. (1). Ibuprofen, furosemide, flurbiprofen, flufenamic acid, griseofulvin, tolbutamide, carbamazepine, clotrimazole and celecoxib showed a maximal aDS below 4 and were deemed as having low potential to supersaturate in this study. Cinnarizine (the time-concentration profiles for this drug are shown in Fig. 1 as an example), albendazole, aprepitant, danazol, felodipine, fenofibrate, itraconazole, ketoconazole and tadalafil were able to supersaturate to a higher degree (aDS = 4–42) and were deemed to having high potential to supersaturate in this study.

It becomes obvious, that investigating a fixed concentration, e.g. 100 mg/ml is not sufficient to readily compare the different drugs (Van Eerdenbrugh et al., 2014). For example, investigations attempting to create an aDS of e.g. 10 corresponding to a concentration of approximately 200 μg/ml for cinnarizine, would mean that the drug would precipitate instantly and thus, would be deemed to having low potential to supersaturate, whereas creating an aDS of e.g. 2 corresponding to approximately 40 μg/ml for cinnarizine, would lead to the opposite conclusion.

A comparison between the potential of the drugs to supersaturate and their respective GFA shows that all nine drugs that supersaturated to a high degree belonged to class 3R with respect to GFA, whilst all drugs belonging to class 2R supersaturated to a low degree. However, ibuprofen, griseofulvin, carbamazepine and clotrimazole which belonged to GFA class 3R only supersaturated to a low degree. It was thus seen that close to 80% of the investigated drugs could be categorized using this threshold of aDS. These findings indicate that drugs which are good glass formers also tendentially have the potential to supersaturate to a high degree.

#### 3.3. Multivariate data analysis

Multivariate data analysis in form of principal component analysis (PCA) was used to further investigate a potential correlation between GFA of a drug and its potential to supersaturate (maximal aDS).

The PCA included the variables: molecular weight, melting point, melt enthalpy, critical cooling rate, classification of GFA (class 1R, class 2R and class 3R), equilibrium solubility and maximal aDS. This resulted in an explained variance of 61% from the first two principal component and a separation of the data set into two subgroups (Fig. 2). The data is

**Table 2**  
Maximal aDS (apparent degree of supersaturation),  $C_{\text{supersaturation}}$  and  $C_{\text{equilibrium}}$  of the investigated drugs.

Drug	GFA class	Maximal aDS	$C_{\text{supersaturation}}$ ( $\mu\text{g/ml}$ )	$C_{\text{equilibrium}}$ ( $\mu\text{g/ml}$ )
Ibuprofen	3R	1	$1876.0 \pm 48.1^b$	$1982.9 \pm 26.5$
Furosemide	2R	1.3	$3734.4 \pm 28.9^b$	$2861.4 \pm 27.1$
Flurbiprofen	2R	1.4	$2222.6 \pm 144.1^b$	$1642.8 \pm 62.9$
Flufenamic acid	2R	1.6	$1298.6 \pm 37.6$	$809.2 \pm 2.6$
Griseofulvin	3R	1.6	$146.8 \pm 2.5$	$89.1 \pm 26.6$
Carbamazepine	3R	2.0	$655.0 \pm 24.8$	$337.5 \pm 9.8$
Tolbutamide	2R	2.1	$2296.3 \pm 89.4$	$1058.2 \pm 26.0$
Clotrimazole	3R	2.2	$99.1 \pm 4.0$	$44.8 \pm 5.9$
Celecoxib	2R	3.1	$211.9 \pm 2.9$	$67.3 \pm 3.8$
Felodipine <sup>a</sup>	3R	4.8	200	$41.2 \pm 0.1$
Cinnarizine	3R	5.4	$112.7 \pm 5.2$	$20.7 \pm 1.4$
Fenofibrate <sup>a</sup>	3R	5.9	89	$14.9 \pm 1.0$
Albendazole <sup>a</sup>	3R	7.4	16	$2.2 \pm 0.1$
Aprepitant <sup>a</sup>	3R	9.9	184	$18.6 \pm 0.8$
Tadalafil <sup>d</sup>	3R	14.5	100	$6.9 \pm 0.2$
Danazol <sup>a</sup>	3R	22.9	80	$3.5 \pm 0.1$
Itraconazole	3R	31.6	$15.8 \pm 0.4$	$0.5 \pm 0.1$
Ketoconazole	3R	42.1	$740.5 \pm 20.1$	$17.6 \pm 2.6$

<sup>a</sup> Data from Palmelund et al. 2016.

<sup>b</sup> No precipitation within 24 h at maximal aDS.

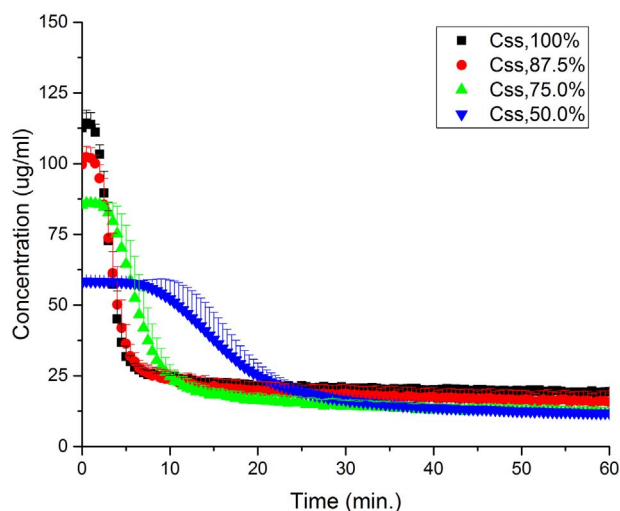


**Fig. 1.** Time-concentration profile of supersaturating cinnarizine using solvent shift from DMSO to fasted state simulated intestinal fluid (FaSSIF).

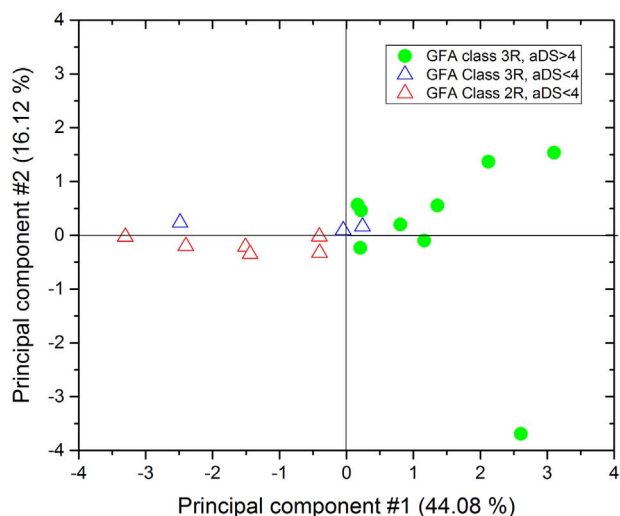


**Fig. 2.** Scores plot of the investigated drugs from principal component analysis.

labeled according to GFA class (2R in red and 3R in green) and potential to supersaturate, i.e. maximal aDS  $\geq 4$  (circles) or aDS  $< 4$  (triangles).

Principal component 1 separated the drugs based on their GFA. The left subgroup mainly consists of GFA class 3R (green) drugs whereas the right subgroup mainly consists of GFA class 2R drugs (red). Furthermore, it was seen that the same subgroups also to a high degree represented the potential to supersaturate, as the left subgroup mainly consists of drugs with a high potential to supersaturate (circles) whereas drugs in the right subgroup can only supersaturate to a low degree (triangles). However, a single observation of a GFA class 3R drug in the right subgroup can be seen, belonging to ibuprofen (Supplementary Fig. S1). This may be explained by its comparatively high equilibrium solubility, which is also situated on the right side in the loading plot (Fig. 3), as nucleation is a stochastic event and with higher equilibrium solubility, more molecules will be available to form nuclei and limit the potential of the drug to supersaturate (Fig. 3). This tendency can also be seen for the remaining drugs investigated in this study, as drugs being able to supersaturate to a high degree generally have lower equilibrium solubility compared to drugs being able to supersaturate to a low degree (Table 2).

The correlation between aDS and GFA can also be seen in the loadings plot from the PCA (Fig. 3), as the two variables cluster closely together. Furthermore, it was found that melt enthalpy is inversely correlated with the potential of the drug to supersaturate (Fig. 3), which was previously found to be a critical physico-chemical properties of good glass formers (Baird et al., 2010; Alhalaweh et al., 2014). The

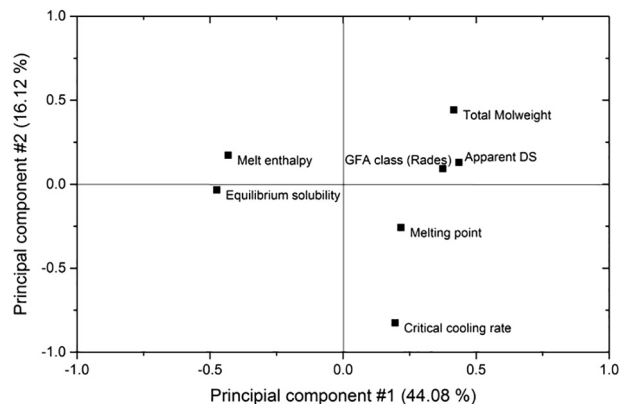


**Fig. 3.** Loadings plot of the investigated drugs from principal component analysis.

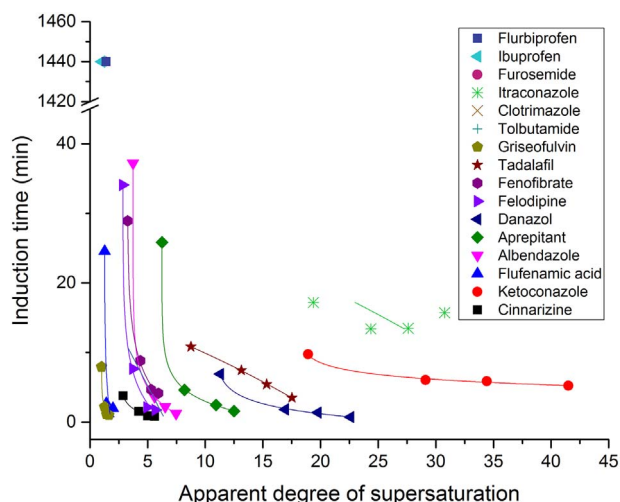


Fig. 4. Relationship between the apparent degree of supersaturation and induction time of the investigated drugs fitted by exponential regression. Celecoxib and carbamazepine are not shown, as the induction time at the four different aDS showed high variance.

melt enthalpy is also part of the Hoffman equation (Eq. (2)) used to calculate the Gibbs free energy between the amorphous and crystalline form (Hoffman, 1958). According to the Hoffman equation, the driving force for crystallization increases with increasing melt enthalpy, and *vice versa* the driving force for crystallization decreases with decreasing melt enthalpy.

### 3.4. Correlation between GFA and time until precipitation

The time until precipitation at four different aDS of the selected drugs was compared using exponential regression between induction time and aDS (Fig. 4). The correlation coefficients ranged from 0.885 (ketoconazole) to 0.973 (danazol) indicating that this method is suitable to compare the investigated drugs.

It was seen that drugs being able to supersaturate to a high degree not necessarily could maintain supersaturation longer at low aDS compared to drugs only being able to supersaturate to a low degree. Four out of five GFA class 2R drugs (celecoxib, flurbiprofen, furosemide and flufenamic acid) could maintain supersaturation at an aDS of 1.5 for longer than 30 min. In contrast, only six out of twelve GFA class 3R drugs (albendazole, aprepitant, danazol, fenofibrate, felodipine and tadalafil) could maintain supersaturation for longer than 30 min at the same aDS. This indicates that GFA of a drug and the time until precipitation at a given aDS may not be correlated.

### 3.5. Discussion of correlations between GFA, aDS and time until precipitation

Several different classification systems of GFA and supersaturation propensity of drugs can be found in the literature. The limited success of correlating these classification systems can be associated with the selected categories used for both GFA and supersaturation propensity (Baird et al., 2010; Van Eerdenbrugh et al., 2014; Raina et al., 2015).

In this study, the inherent GFA has been determined in form of the critical cooling rate or minimal milling time in contrast to the GFA determined by the recrystallization of a drug during predetermined heating and cooling cycles. Furthermore, in contrast to using a fixed DS for all drugs, the inherent potential of the drug to supersaturate was determined by the use a solvent shift method based on the maximal drug concentration before precipitation. A tendency was seen that drugs having a high potential to supersaturate also are good glass formers and drugs only being able to supersaturate to a low degree are poor glass formers. In contrast, a similar correlation was not found

between GFA and time until precipitation at a given aDS.

These results may be explained by the potential of a drug to supersaturate being governed by its solid state properties including glass forming ability and melt enthalpy. In contrast, the time until precipitation at a given aDS may be governed by the solution properties of the drug and thus no correlation with GFA (a solid state property) should be expected.

## 4. Conclusion

In this study, the inherent glass forming ability (GFA) of 23 different drugs was determined via either melt quenching or milling. Additionally, the inherent supersaturation propensity of the selected drugs was determined by a  $\mu$ -dissolution set-up using solvent shift to induce supersaturation. The GFA of the drugs was successfully classified according to a previously developed classification system with five drugs belonging to class 1R, five drugs belonging to class 2R and the remaining thirteen drugs belonging to class 3R. Furthermore, the inherent supersaturation propensity was successfully determined by the use of a solvent shift method and differentiated in this study into maximal aDS and time until precipitation at a given aDS. A correlation between a GFA and maximal aDS was found. Multivariate data analysis also revealed that GFA and the potential to supersaturate of a drug are indeed correlated. The analysis further showed that the physico-chemical property melt enthalpy is inversely correlated with the potential to supersaturate and form a glass. No correlation could be established between GFA and its time until precipitation at a given aDS in this study. An amorphous drug will rarely be formulated in its pure form, but rather as a glass solution. Future studies will therefore investigate the translational effect of this study to drug-polymer combinations, as the addition of polymers can inhibit precipitation and increase solubility of a drug.

## Acknowledgements

This work was supported by Actelion Pharmaceuticals Ltd. – Switzerland and Idorsia Pharmaceuticals Ltd. – Switzerland. We would like to thank Markus von Raumer and Céline Lienhart from Idorsia Pharmaceuticals Ltd. and Rassul Hussain Ali Al Salman from Department of Pharmacy at University of Copenhagen for valuable discussions during this study.

## Appendix A. Supplementary data

Supplementary data associated with this article can be found, in the online version, at <http://dx.doi.org/10.1016/j.ijpharm.2018.01.013>.

## References

- Di, L., Kerns, E.H., Carter, G.T., 2009. Drug-like property concepts in pharmaceutical design. *Curr. Pharm. Des.* 15 (19), 2184–2194.
- Kalepu, S., Nekkanti, V., 2015. Insoluble drug delivery strategies: review of recent advances and business prospects. *Acta Pharm. Sin. B* 5 (5), 442–453.
- Hancock, B.C., Parks, M., 2000. What is the true solubility advantage for amorphous pharmaceuticals? *Pharm. Res.* 17 (4), 397–404.
- Baird, J.A., Van Eerdenbrugh, B., Taylor, L.S., 2010. A classification system to assess the crystallization tendency of organic molecules from undercooled melts. *J. Pharm. Sci.* 99 (9), 3787–3806.
- Blaabjerg, L.I., Lindenberg, E., Löbmann, K., Grohgan, H., Rades, T., 2016. Glass forming ability of amorphous drugs investigated by continuous cooling and isothermal transformation. *Mol. Pharm.* 13 (9), 3318–3325.
- Blaabjerg, L.I., Lindenberg, E., Rades, T., Grohgan, H., Löbmann, K., 2017. Influence of preparation pathway on the glass forming ability. *Int. J. Pharm.* 521 (1–2), 232–238.
- Guzman, H.R., Tawa, M., Zhang, Z., Ratanabanangkoon, P., Shaw, P., Gardner, C.R., et al., 2007. Combined use of crystalline salt forms and precipitation inhibitors to improve oral absorption of celecoxib from solid oral formulations. *J. Pharm. Sci.* 96 (10), 2686–2702.
- Palmelund, H., Madsen, C.M., Plum, J., Müllertz, A., Rades, T., 2016. Studying the propensity of compounds to supersaturate: a practical and broadly applicable approach. *J. Pharm. Sci.* 105 (10), 3021–3029.
- Sudha, C., Srinivasan, K., 2013. Supersaturation dependent nucleation control and

- separation of mono, ortho and unstable polymorphs of paracetamol by swift cooling crystallization technique. *CrystEngComm* 15 (10), 1914–1921.
- Tian, F., Sandler, N., Gordon, K., McGoverin, C., Reay, A., Strachan, C., et al., 2006. Visualizing the conversion of carbamazepine in aqueous suspension with and without the presence of excipients: a single crystal study using SEM and Raman microscopy. *Eur. J. Pharm. Biopharm.* 64 (3), 326–335.
- Gao, P., Shi, Y., 2012. Characterization of supersaturatable formulations for improved absorption of poorly soluble drugs. *AAPS J.* 14 (4), 703–713.
- Li, P., Vishnuvajjala, R., Tabibi, S.E., Yalkowsky, S.H., 1998. Evaluation of in vitro precipitation methods. *J. Pharm. Sci.* 87 (2), 196–199.
- Wu, H., Khan, M.A., 2011. Quality-by-design: an integrated process analytical technology approach to determine the nucleation and growth mechanisms during a dynamic pharmaceutical coprecipitation process. *J. Pharm. Sci.* 100 (5), 1969–1986.
- Karmwar, P., Graeser, K., Gordon, K.C., Strachan, C.J., Rades, T., 2011. Investigation of properties and recrystallisation behaviour of amorphous indomethacin samples prepared by different methods. *Int. J. Pharm.* 417 (1), 94–100.
- Karmwar, P., Graeser, K., Gordon, K.C., Strachan, C.J., Rades, T., 2012. Effect of different preparation methods on the dissolution behaviour of amorphous indomethacin. *Eur. J. Pharm. Biopharm.* 80 (2), 459–464.
- Ozaki, S., Minamisono, T., Yamashita, T., Kato, T., Kushida, I., 2012. Supersaturation–nucleation behavior of poorly soluble drugs and its impact on the oral absorption of drugs in thermodynamically high-energy forms. *J. Pharm. Sci.* 101 (1), 214–222.
- Van Eerdenbrugh, B., Raina, S., Hsieh, Y.-L., Augustijns, P., Taylor, L.S., 2014. Classification of the crystallization behavior of amorphous active pharmaceutical ingredients in aqueous environments. *Pharm. Res.* 31 (4), 969–982.
- Van Speybroeck, M., Mols, R., Mellaerts, R., Do Thi, T., Martens, J.A., Van Humbeeck, J., et al., 2010. Combined use of ordered mesoporous silica and precipitation inhibitors for improved oral absorption of the poorly soluble weak base itraconazole. *Eur. J. Pharm. Biopharm.* 75 (3), 354–365.
- Mullin, J.W., Söhnel, O., 1977. Expressions of supersaturation in crystallization studies. *Chem. Eng. Sci.* 32 (7), 683–686.
- Murdande, S.B., Pikal, M.J., Shanker, R.M., Bogner, R.H., 2010. Solubility advantage of amorphous pharmaceuticals: II. Application of quantitative thermodynamic relationships for prediction of solubility enhancement in structurally diverse insoluble pharmaceuticals. *Pharm. Res.* 27 (12), 2704–2714.
- Murdande, S.B., Pikal, M.J., Shanker, R.M., Bogner, R.H., 2011. Solubility advantage of amorphous pharmaceuticals, part 3: is maximum solubility advantage experimentally attainable and sustainable? *J. Pharm. Sci.* 100 (10), 4349–4356.
- Almeida e Sousa, L., Reutzel-Edens, S.M., Stephenson, G.A., Taylor, L.S., 2015. Assessment of the amorphous “Solubility” of a group of diverse drugs using new experimental and theoretical approaches. *Mol. Pharm.* 12 (2), 484–495.
- Hoffman, J.D., 1958. Thermodynamic driving force in nucleation and growth processes. *J. Chem. Phys.* 29 (5), 1192–1193.
- Raina, S.A., Eerdenbrugh, B.V., Alonzo, D.E., Mo, H., Zhang, G.G., Gao, Y., et al., 2015. Trends in the precipitation and crystallization behavior of supersaturated aqueous solutions of poorly water-soluble drugs assessed using synchrotron radiation. *J. Pharm. Sci.* 104 (6), 1981–1992.
- Augustijns, P., Wuyts, B., Hens, B., Annaert, P., Butler, J., Brouwers, J., 2014. A review of drug solubility in human intestinal fluids: implications for the prediction of oral absorption. *Eur. J. Pharm. Sci.* 57, 322–332.
- Fagerberg, J.H., Karlsson, E., Ulander, J., Hanisch, G., Bergström, C.A., 2015. Computational prediction of drug solubility in fasted simulated and aspirated human intestinal fluid. *Pharm. Res.* 32 (2), 578–589.
- Alhalaweh, A., Alzghoul, A., Kaialy, W., Mahlin, D., Bergström, C.A., 2014. Computational predictions of glass-forming ability and crystallization tendency of drug molecules. *Mol. Pharm.* 11 (9), 3123–3132.